# BINARY DIAMONDOID MOLECULAR GELS

BY

MENGWEN ZHANG

THESIS

Submitted in partial fulfillment of the requirements
for the degree of Master of Science in Chemical Engineering
in the Graduate College of the
University of Illinois at Urbana-Champaign, 2013

Urbana, Illinois

Advisor:

Professor Charles F. Zukoski

## ABSTRACT

We demonstrate the formation of gels composed of saturated carbon cage, diamondoid molecules that are rendered attractive through acid-base, non-covalent interactions (hydrogen bonding either with or without proton transfer). The gels are formed by mixing dimethyl sulfoxide (DMSO) solutions of 1-adamantanecarboxylic acid (A1C) with 1-adamantylamine (A1N). Upon mixing at vanishing concentrations, these diamondoid molecules rapidly aggregate. At approximately 3% by weight, the resulting suspension forms a percolated network. These resulting gels have elastic moduli of $10^2$-$10^4$Pa at diamondoid concentrations in the 3-7wt% range. With increasing applied stress these gels yield and shear thin. Upon cessation of the applied stress, the gels recover their quiescent properties and demonstrate reversibility. At 1:1 mole ratio of 1-adamantanecarboxylic acid (A1C) and 1-adamantylamine (A1N), the gel's elastic modulus increases as $\phi^x$ with x~4. Transmission Electron Microscope (TEM) images indicate that the gels are formed from a network of interwoven and branched fibers. In combination, the flow properties and TEM images indicate that the fibers can be broken down under shear and reform in the absence of shear. Both Wide-angle and Small-angle X-ray Scattering (WAXS and SAXS) are used to investigate the gel's microstructure. Particular attention is paid to determine the applicability of models for colloidal gelation to these molecular gels.

**ACKNOWLEDGMENTS**

First of all, I would like to express my sincere appreciation to my advisor, Charles F. Zukoski, for guiding me through my Masters at UIUC. Under his guidance, I am able to learn about a wonderful field of science that was completely new to me. In addition, I would like to thank all of my lab mates for all the useful suggestions on my research. Finally, I would like to thank Danielle Gray, director of George L. Clark X-Ray Facility at Noyes Laboratory, for assisting me with data acquisition and analysis.

This material is based on work supported by the U.S. Department of Energy, Division of Materials Science under Award No.DE-FG02-07ER4471, through the Frederick Seitz Materials Research Laboratory at the University of Illinois Urbana-Champaign. Research in this work was carried out in part in the Frederick Seitz Materials Research Laboratory Central Facilities, University of Illinois University, which are partially supported by the U.S. Department of Energy under grants DE-FG02-07ER46453 and DE-FG02-07ER46471.

## TABLE OF CONTENTS

# CHAPTER 1. INTRODUCTION

## 1.1 Overview

Gels are used in almost every aspect of our life from things such as food products (Jell-O and syrups) to personal care products (shampoo and toothpaste), and have many applications in the biomedical field and the pharmaceuticals.[1] While these materials are an essential part of our life, they are often poorly characterized. To better understand gels, we will first ask ourselves the question of "what is a gel?" In scientific terms, according to Weiss et al., two characteristics define a gel: i) it exhibits solid-like rheological behaviors at low applied stress even though it contains mostly liquid; and ii) it has "a continuous microscopic structure with macroscopic dimension that is permanent on the time scale of analytical experiment."[1] Simply put, a gel is mostly liquid but behaves like a solid; it is a system that supports its own weight over a time scale of importance for the use of the gel or the observation of its properties. The main types of gels are: polymeric gels, colloidal gels, and molecular gels. The first two types of gels have been studied in-depth and have been widely used in consumer products; in the last decade or so, molecular gels are seeing an increasing significance.

The formation of molecular gels involves two essential components: the solvent and the gelator molecules. Molecular gels are a type of physical gel that utilizes non-covalent interactions for self-assembly. Examples of such interactions are: hydrogen bonding, π-π interactions. hydrophobic interactions, van der Waals, and metal-ligand coordination.[2] The resulting self-assembly is usually fibrous in

nature; however, other geometry such as ribbons and sheets do exist.[1] Molecular gels are often formed at a very low weight percent of gelator molecules in solution.[1]

Molecular gels have several unique properties that make them promising for future applications in a variety of fields. For instance, the non-covalent bonds render molecular gels sensitive to stimuli such as temperature, light, pH, and other solution conditions. Thus, they are ideal for use in stimuli-responsive materials such as sensors and actuators.[2,3] In addition, these gels have self-healing and recovery capabilities that make them promising for use in biomaterials. Because of the structural diversity of these gels, it is possible to use them as templates for creating inorganic or organic nanostructures that are used in separation and catalysis.[3] In addition, proposed applications of molecular gels include drug delivery, oil recovery, electronic materials, and liquid crystalline materials.[2,3]

Many molecular gels are often discovered by serendipity. As a result, there are many ongoing efforts aimed at understanding the gelation mechanisms and designing new gelating molecules. Parameters such as the ease of crystallization and solubility of the gelating molecules have been explored in-depth to understand the gelating mechanisms. [3] My thesis can be viewed as an attempt to build deeper understanding of molecular gel formation from a different perspective: from our understandings of colloidal gels.

The molecule of interest for my thesis is adamantane, which is composed of saturated hydrocarbon in a cage-like structure.[4] This molecule is the simplest diamondoid in existence. Diamondoids have already been widely-used in applications in material science: they have been used in polymer synthesis to

increase thermal stability of the polymer, in crystal engineering, in biopolymers to add stiffness to the system, and in producing highly diverse and symmetrical nanostrucutres for applications in nanotechnology.[4] Besides the unique properties of diamondoids mentioned above, we are mainly interested in this particular molecule because of its globular shape and resemblance to colloidal particles. We anticipate interesting and unique rheological and even possibly structural properties that are similar to those of colloidal gels.

Thus, the purpose of my thesis is to first, experiment with different adamantane molecules to find one that gels, and then, to compare the rheological behaviors of this system with known colloidal system. We hypothesize that other than the obvious size differences, (molecules in Å, colloids in μm), their rheological properties may be surprisingly similar. My thesis will explore this idea in the next two chapters, with Chapter 1 describing a model molecular system, and Chapter 2 analyzing the rheological and structural properties of the molecular system and comparing it to colloidal systems.

### 1.2 References

(1) Weiss, R.G.; Terech, P. *Molecular Gels: Materials with Self-Assembled Fibrillar Networks.* Springer: Dordrecht, The Netherlands. **2006**.

(2) Buerkle, L., Rowan, S.J., Supramolecular gels formed from multi-component low molecular weight species. *Chem. Soc. Rev.* **2012.** 41, 6089-6102.

(3) Sangeetha, N. M.; Maitra, U. Supramolecular gels: Functions and uses. *Chem. Soc. Rev.* **2005**, *34***,** 821-836.

(4) Mansoori, G.A., de Araujo, P.L.B., de Araujo, E.S., *Diamondoid Molecules, with Applications in Biomedicine, Materials Science, Nanotechnology & Petroleum Science.* World Scientific Publishing Co. Pte. Ltd. Singapore. 2012.

## CHAPTER 2. BINARY DIAMONDOID MOLECULAR GELS

### 2.1 Introduction

Molecular gels have received much attention in the last decade as a type of molecular self-assembly.[1,2] Often the gels are composed of fibrillar networks that form at very low concentrations and have potential applications in chemical sensing,[3,4] oil recovery,[5] regenerative medicine,[6,7] and the construction of optical devices.[5] Of particular interest is the ability of some molecules to form soft materials at low concentration of $\leq$ 2 wt. % of gelator molecules in an appropriate solvent. [2] These soft materials are space filling and have long relaxation times such that they are elastic and have yield stresses when probed at short time scales and typically shear thin with increasing applied stress. The molecules which compose the gel interact via non-covalent forces such as H-bonding, π-π stacking, van der Waals, dipole-dipole, and coordination interactions to form a network that entraps the solvent. Because of interaction via physical forces, many molecular gels are thermally reversible. [5]

In recent years, many efforts have been placed on designing molecular gelators.[8-10] This is now known to be a surprisingly complicated task with similar molecular structures displaying very different states of solution aggregation.[11,12] Gelation is associated with driving the molecule close to or crossing a solubility boundary where the strength of molecular attractions is sufficient to drive self-assembly and aggregation.[8] As a result, three possible states of molecular association are often reported: (i) amorphous precipitation where the molecules pass through a solubility boundary and precipitate as

amorphous solids, (ii) crystallization where the molecules assemble into well-ordered crystals that are discrete objects (i.e., not space filling), and (iii) gelation, where the degree of order in the resulting structure is complicated and often referred to as an intermediate between precipitation and crystallization.[5] Unlike crystals or precipitates, gels are space-filling structures and can be composed of regular- perhaps crystalline- order at small length scales or they can be composed of amorphous molecular packing. The key element for gel formation is the formation of extended structures such as fractal aggregates or branched fibers.

In this paper we introduce a novel two-component molecular gel composed of cage-like adamantane molecules with a size of approximately 0.6 nm.[13] Our interest in these molecules is derived from the particulate nature of the molecular core and interest in comparing gel formation in molecular systems with gel formation in colloidal and nanoparticle systems. These cage molecules are composed of saturated hydrocarbon structures and are referred to as being diamondoid in nature. In this case, we choose two molecules: an amino and a carboxylate derivative of the same adamantane cage. These molecules are soluble in polar aprotic media due to an attached polar group. When mixed, we believe that non-covalent acid-base interactions (hydrogen bonding) and van der Waals forces would drive the cage molecules together. In Section 2.2, we discuss our experimental system and methods of characterization; in Section 2.3, we describe gel formation and mechanics and the use of TEM and DLS (dynamic

light scattering) to characterize the properties of the resulting gels. In Section 2.4 we present our conclusions.

## 2.2 Experimental Section

**Materials.** The gelators 1-adamantanecarboxylic acid ($C_{11}H_{16}O_2$) and 1-adamantylamine ($C_{10}H_{17}N$) were acquired from Sigma Aldrich (Figure 1). Both molecules have a diamond-like caged molecular structure.[14] Reagent grade DMSO (>99.9%) from Fisher Scientific was used as the solvent.

**Preparation of gels.** Stock solutions of 1-adamantanecarboxylic (A1C) and 1-adamantylamine (A1N) in DMSO were prepared individually. Each solution was heated at 70$^{o}$C for 20 minutes until all the gelators had dissolved completely. The solutions were then cooled to room temperature and checked for clearness. The stock solutions were then diluted to lower concentrations. To produce gels, solutions of A1C and A1N were rapidly mixed together for 30 seconds using a Thermolyne mixer.

**Rheology.** Rheology measurements were performed using Bohlin rheometer at room temperature. A cone-and-plate geometry (CP $4^{o}$/40mm) with a gap space of 150mm was employed. To investigate the effect of gelator concentration on rheology, the gels were prepared by mixing equimolar amounts of A1N and A1C at various concentrations. Amplitude sweep tests were performed at a frequency of 1Hz at room temperature to measure the gel's elastic modulus ($G'$) and viscous modulus ($G''$) as a function of shear stress ($\sigma$). The gels were pre-sheared manually at first to remove heterogeneity from the sample. Amplitude sweeps were then performed three times for each sample.

The linear elastic moduli ($G_o'$), linear viscous moduli ($G_o''$), and yield shear stress ($\sigma_y$) were determined in these experiments. At the yield stress $\sigma_y$, elastic modulus equals to viscous modulus (G'=G") and the sample transforms from a solid-like (G'>G") state to a liquid-like (G'<G") state. Frequency sweeps were performed at each concentration to gauge the dependence of moduli on frequency.

**Dynamic Light Scattering (DLS).** In order to characterize the size of the fundamental units within the gel, DLS was carried out using FOQELS Particle Size Analyzer at room temperature. Gels at several gelator concentrations (1wt%, 3wt%, 5wt%) were tested and the average effective size was reported at each concentration. Because of the opaque nature of these gels, each sample was diluted down to 0.1wt% before DLS was performed.

**TEM.** A 3wt% gel prepared by mixing equimolar amounts of A1N and A1C was made and then diluted down to 1wt%. A 200 mesh Cu holey-carbon grid from SPI Supplies was dipped into the diluted gel for 10 seconds and place onto a glass slide. The sample was dried overnight. TEM images were acquired using JOEL 2100 Cryo TEM at 200kV and captured by DigitalMicrograph Software (Gatan).

### 2.3 Results and Discussion

**Description of the Gel.** Immediately after the addition of the clear and colorless A1C solution to the clear and colorless A1N solution, the system turns turbid, indicating formation of aggregates with sizes greater than 100nm (Figure 2b). A simple inverted-bottle test suggests that the gel point is at

approximately 3wt% (Fig. 2c). However, even at concentrations below the gel point, the solution rapidly becomes turbid upon mixing of A1C with A1N.

After inverting a gel for a while, DMSO was observed to drain out gradually from the gel network. While the initial gel will have a DMSO volume fraction, $\phi_{DMSO} = 0.97$, the gel drains until $\phi_{DMSO} \sim 0.85$. This indicates that the initial gel network is weak and is readily compressed by capillary forces.

**Rheology.** The gel is characterized by its elastic modulus ($G'$), linear viscous modulus ($G''$), and yield shear stress ($\sigma_y$). While the elastic modulus is a measure of the ability of a deformed object to store energy when subjected to deformation, the viscous modulus measures the dissipation of energy when subjected to a stress. The yield stress characterizes the stress where the gel breaks and starts to flow. Figure 3 shows a characteristic amplitude sweep of gels formed from an equimolar mix of A1N and A1C at 3wt%, 5wt%, and 7wt%, respectively. With increasing stress amplitude, the moduli initially show linear responses and at higher stresses, the samples display characteristics of colloidal gels where there is first a roll-off in $G'$ and then in $G''$. Subsequently, at the yield stress $\sigma_y$, $G'$ crosses $G''$, indicating that the gel structure is disrupted at this stress.[15] Linear elastic moduli $G_o'$ and linear viscous moduli $G_o''$ are determined at low stress amplitudes where the moduli are independent of the stress amplitude. Figure 3 suggests that the linear elastic modulus $G_o'$ increases approximately two orders of magnitudes from $10^2$ Pa at 3wt% to $10^4$ Pa at 7wt%. The yield stress $\sigma_y$ also increases with an increase in concentration. Amplitude sweeps were carried out at least three times successively at each

concentration where the gel is fully disrupted $G'' >> G'$. The values of the modulus curves were reproducible each time, suggesting that the gels rapidly recover after shear. Over a strain frequency range of 0.1-10 Hz, moduli were observed to be independent of strain frequency. Figure 4 shows the frequency sweep for gels at concentrations of 3wt% and 7wt%. The lack of dependence on frequency suggests the structures in the gel rearrange slowly with time constant greater than 10s.

**TEM and DLS.** As shown by the TEM images, the gel is composed of expanded fibrillar networks (Figure 5a, 5b). The diameters of the fibers vary from very thin strands of 200 nm to large bulky ones of $\geq$1μm. Dynamic Light Scattering (DLS) also suggests the presence of large structures with size of 1-2μm inside the gel.

**Electron Diffraction.** Previous studies have shown that by using a different synthesis method, single crystals of adamantan-1-ammonium 1-adamantanecarboxylate ($C_{21}H_{33}NO_2$), which consists of a 1-adamantylammonium cation and a 1-adamantane carbonyloxy anion, have been formed.[16] Thus, to check whether crystals also exist in these fibers, electron diffraction patterns were collected. The diffraction peaks for single crystals of adamantan-1-ammonium 1-adamantanecarboxylate ($C_{21}H_{33}NO_2$) have been carefully marked in black on Figure 6a. However, as observed in Figure 6, no spotty rings or ordered spots typical of crystalline structures have been detected in the pattern. The marked peak positions for single crystal data of adamantan-1-ammonium 1-adamantanecarboxylate ($C_{21}H_{33}NO_2$) are not clearly observed in

the electron diffraction patterns of single gel fibers such as that shown in Figure 6a. This suggests that the system either does not have long-range order and is amorphous, or contains randomly oriented nanosized crystallites. To further resolve the internal structure of this gel, wide-angle x-ray scattering will be subsequently performed.

## 2.4 Conclusion

In this chapter, we demonstrate the formation of gels composed of diamondoid molecules of 1-adamantylamine and 1-adamantanecarboxylic acid in DMSO. The gels form at 3% by weight for a 1:1 mixture of these molecules. TEM and DLS indicate the formation of large fibrous structures with diameters and lengths ranging from several hundred nanometers to $\geq$ 1 μm. The gels are mechanically reversible in that they can be sheared at a high shear rate to a low viscosity and, upon cessation of shear, the structure and mechanical properties recover. In addition, while the gels are composed of structures of sufficiently strong bonds that have relaxation times of longer than 10 s, they are sufficiently weak that they will collapse as solvent drains from them.

Unlike typical molecular gelators that have expanded chemical structures with multiple aromatic rings for π-π stacking and are capable of forming many bonds with the neighboring molecules, this novel binary gel is composed of small and compact, almost colloid-like, diamondoid molecules with limited number of bonds. Future work will further explore: i) how aggregates of these binary pairs assemble into nanocrystalline or amorphous aggregates with well defined elongated structures, ii) the rheological behavior of this binary gel.

## 2.5 Tables and Figures

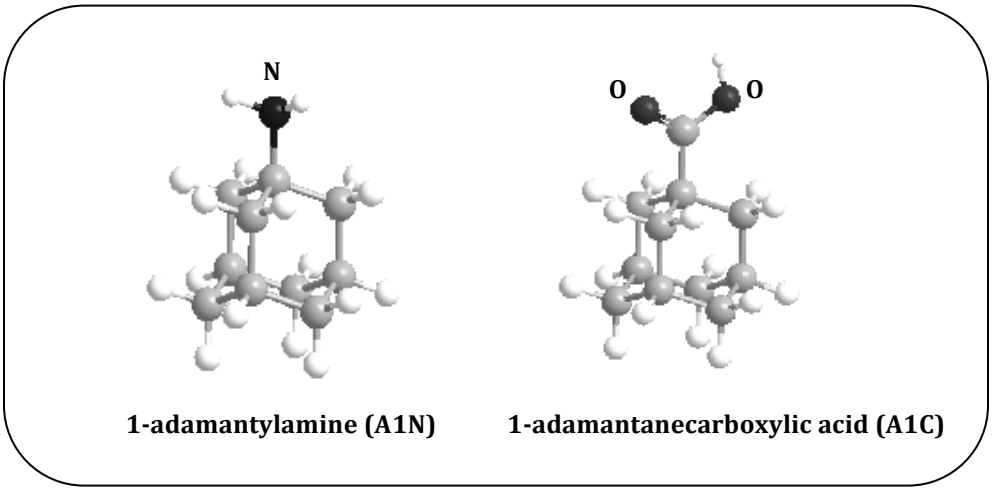


**Figure 1.** 3-D representations of 1-adamantylamine (A1N) and 1-adamantane-carboxylic acid (A1C) (C: gray; H: white, N or O: Black).

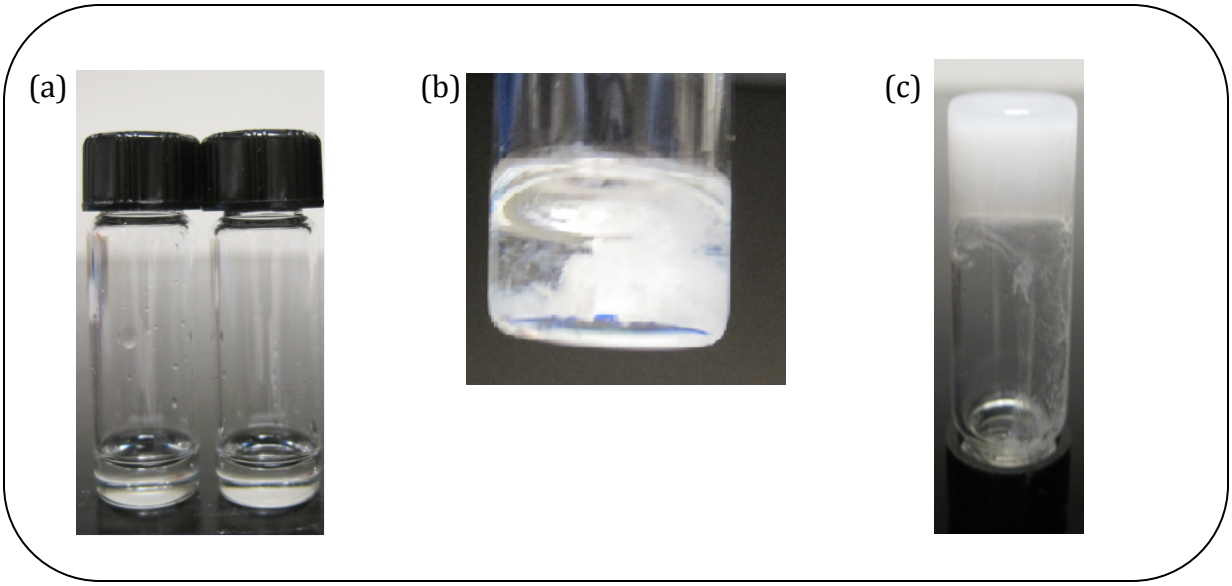


**Figure 2.** (a) Clear solution of A1N (left) and A1C (right) at 3wt% in DMSO. (b) Solution right after mixing of A1N and A1C. (c) Inverted bottle test after 30 seconds of mixing.

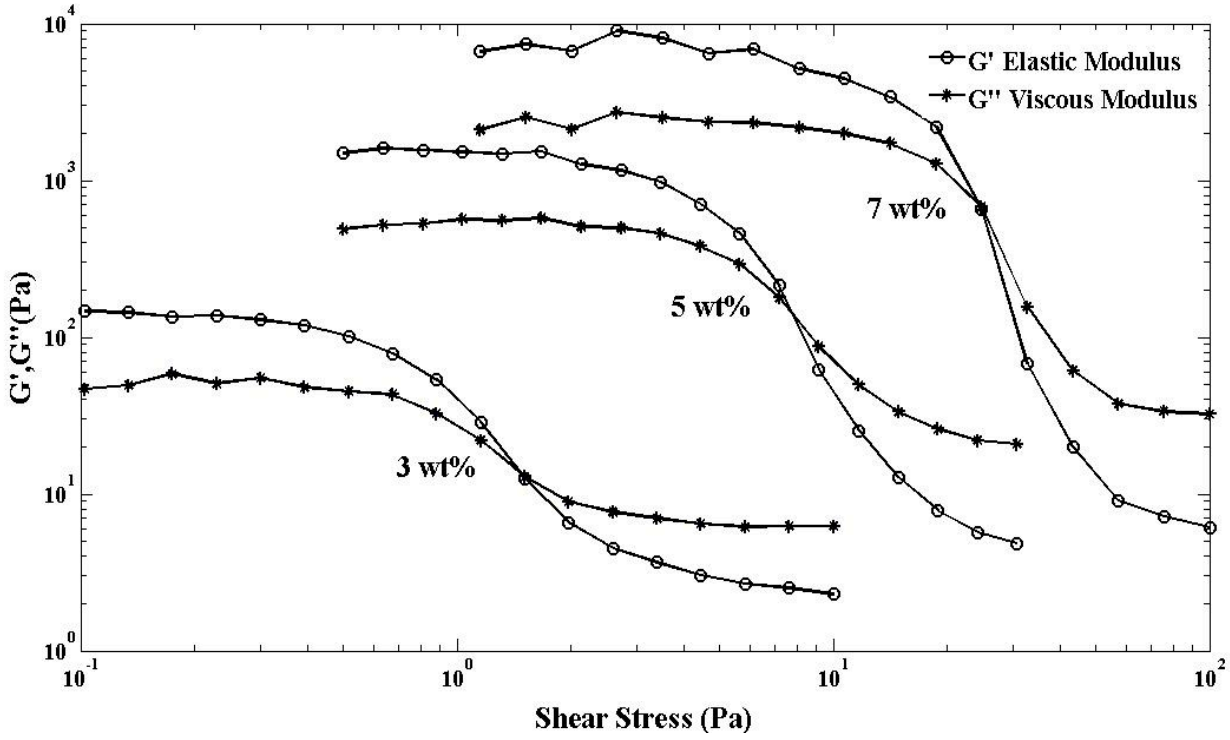


**Figure 3.** Elastic modulus ($G'$) and viscous modulus ($G''$) measured at 1Hz plotted as a log-log function of shear stress ($\sigma$) for a 3wt%, 5wt%, and 7wt% equimolar gel.

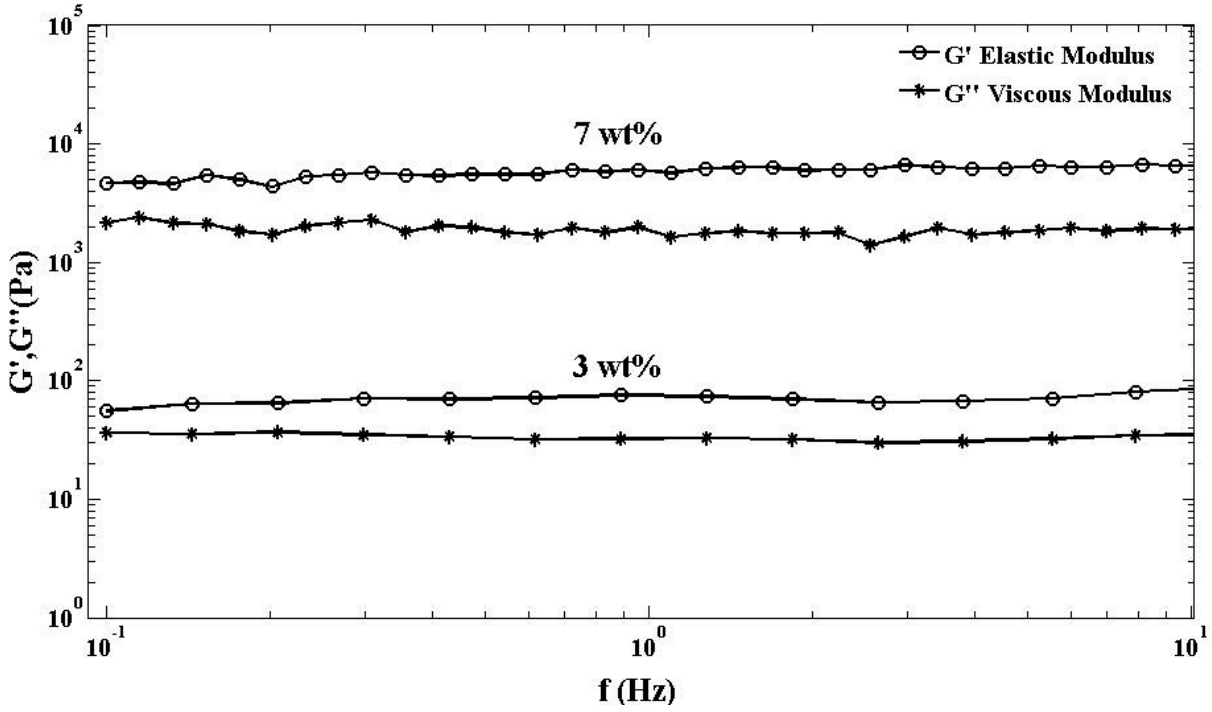


**Figure 4.** Frequency sweep for 3wt% and 7wt% gels respectively from 0.1 to 10 Hz.

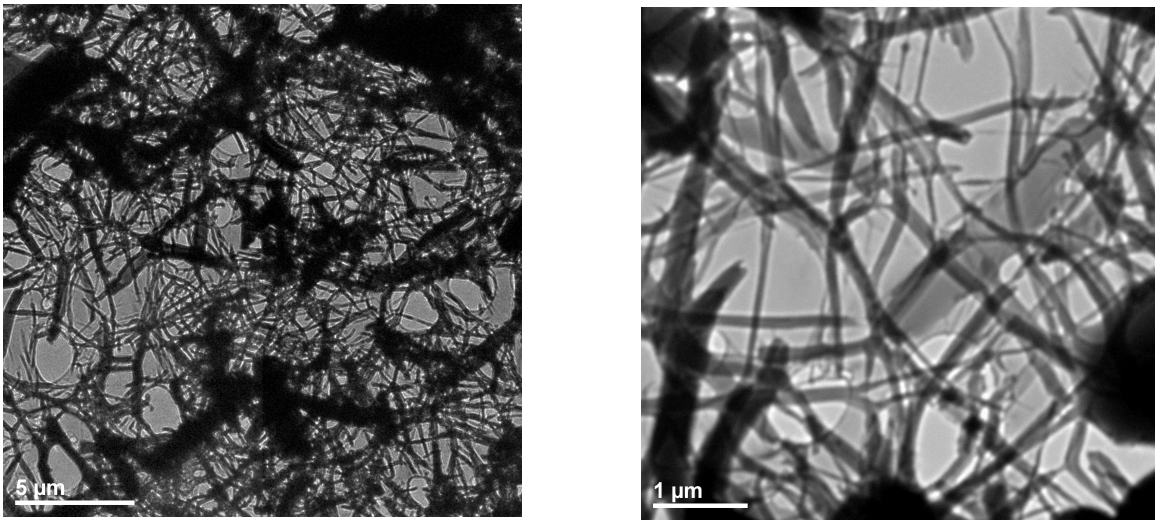


**Figure 5.** (a) TEM showing the fibrous network of the gel. (b) Slightly enlarged view of the fiber network.

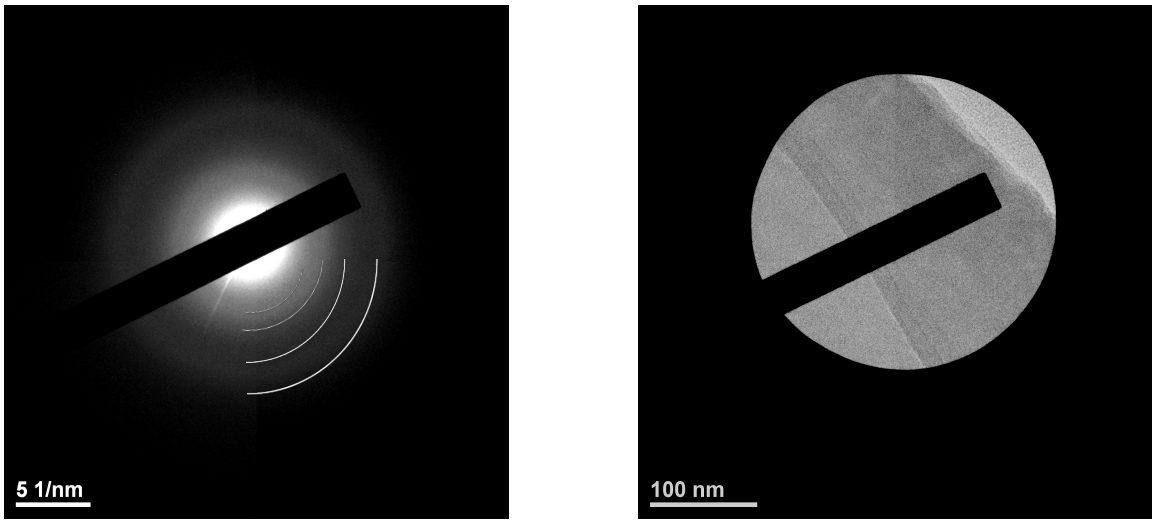


**Figure 6.** (a) Electron diffraction pattern for a specific fiber in the gel. (b) A section of the fiber on which electron diffraction is performed.

## 2.6 References

(1) Smith, D. K. Molecular Gels-Nanostructured Soft Materials. In *Organic nanostructures;* Steed, J. W., Atwood, J. L., Eds.; Wiley-VCH: Weinheim, Germany. **2008**, 111-154.

(2) Weiss, R.G.; Terech, P. *Molecular Gels: Materials with Self-Assembled Fibrillar Networks.* Springer: Dordrecht, The Netherlands. **2006**.

(3) Kim, T. H.; Kim, D. G.; Lee, M.; Lee, T. S. Synthesis of reversible fluorescent organogel containing 2-(2'-hydroxyphenyl)benzoxazole: fluorescence enhancement upon gelation and detecting property for nerve gas simulant. *Tetrahedron* **2010**, *66(9),* 1667-1672.

(4) Chen, J.; McNeil, A. J. Analyte-Triggered Gelation: Initiating Self-Assembly via Oxidation-Induced Planarization. *J. Am. Soc. Chem.* **2008**, *130(49)*, 16496-16497.

(5) Sangeetha, N. M.; Maitra, U. Supramolecular gels: Functions and uses. *Chem. Soc. Rev.* **2005**, *34***,** 821-836.

(6) Webber, M. J.; Kessler, J. A.; Stupp, S. I. Emerging peptide nanomedicine to regenerate tissues and organs. *J. Intern. Med.* **2010***, 267, 71-88.*

(7) Jung, J. P., Nagaraj, A. K., Fox E. K., Rudra, J. S., Devgun, J. M.; Collier, J. H. Co-assembling peptides as defined matrices for endothelial cells. *Biomaterials,* **2009**, *30(12)*, 2400-2410.

(8) van Esch, J. H.; We can Design Molecular Gelators, But Do We Understand Them? *Langmuir* **2009,** *25(15),* 8392-8394.

(9) Muro-Small, M. L.; Chen, J.; McNeil, A. J. Dissolution Parameters Reveal Role of Structure and Solvent in Molecular Gelation. *Langmuir,* **2011**, *27(21),* 13248-13253.

(10) Dastidar, P. Supramolecular gelling agents: can they be designed? *Chem. Soc. Rev.* **2008**, *37*(12), 2699-2715.

(11) Ma, M.; Kuang, Y.; Gao, Y.; Zhang, Y.; Gao, P.; Xu, B. Aromatic-Aromatic Interactions Induce the Self-Assembly of Pentapeptidic Derivatives in Water To Form Nanofibers and Supramolecular Hydrogels. *J. Am. Chem. Soc.* **2010**, *132*, 2719-2728.

(12) Karthik Kumar, K.; Elango, M.; Subramanian, V.; Mohan Das, T. Novel-saccharide-pyridine based gelators: selective gelation and diversity in superstructures. *New J. Chem.* **2009**, *33,* 1570-1577.

(13) Morel, J.-P.; Morel-Desrosiers, N. Standard Molar Enthalpies and Volumes of Adamantane in Methanol, Ethanol, Acetone, and n-Dodecane. Interpretation using Scaled Particle Theory. *J. Solution Chem.* **1981**, *10(6),* 451-458.

(14) Ermer, O. Fivefold-Diamond Structure of Adamantane-1,3,5,7, Tetracarboyxlic Acid. *J. Am. Chem. Soc.* **1988,** *110(12),* 3747-3754.

(15) Mewis, J.; Wagner, N. J. *Colloidal Suspension Rheology*. Cambridge University Press: New York, U.S., **2012**, 206-217.

(16) Mullica, D. F.; Scott, T. G.; Farmer, G. M.; Kautz, J. A.; Structure of adamantan-1-ammonium 1-adamantanecarboxylate. *J. Chem. Crystallogr.* **1999**, *29(7),* 845-848.

# Chapter 3. An Analysis on the Novel Structural and Rheological Properties of A Binary Diamondoid Molecular Gel

## 3.1 Introduction

In the last decade, with the advance of technology, there has been growing interest in self-assembly of nano-structures. Molecular gels assembled from small molecules are one example of such structures. Until the present, most molecules that form gels have been discovered serendipitously. Conditions that result in assembly of these space-filling structures are poorly understood.

Colloidal gels, composed of spherical particles in the nanometer and larger size region have been studied for decades and the conditions that give rise to gelation are well understood. Gelation is associated with particles that are localized by attractive interactions. If the particles are sufficiently monodisperse, gelation often occurs under conditions where the lowest free energy of the system exists for particles assembled into crystals. Thus gels, the formation of space-filling networks of localized particles with limited long-range order, are only metastable states. Crystallization can be eliminated if the particles have a size distribution with a standard deviation of greater than ~8% of the modal size. Under these conditions, there is debate if the gel is the lowest free energy state or if gels represent an arrested gas-liquid phase transition.[1]

Colloidal gels systems are analogous to molecular gel systems, except that the absolute sizes of the particles forming the network are substantially larger. Of particular interest to us are how and in what fashion are these two systems comparable to and/or different from each other?

For typical colloidal gels, the gelling colloidal particles can be treated as globular objects experiencing centro-symmetric attractions. The strength of attractions can be tuned through alterations of solution conditions such as pH, ionic strength, or the concentrations of non-absorbing polymer. Recently, there has been interest in forming colloidal gels by introducing anisotropic interactions.[2,3] Anisotropy can be controlled by the number of attractive bonds or 'hotspots' on the colloidal particles. One of the successful efforts in fabricating such anisotropic colloidal particles has been realized by Wang et al. recently.[4] Our group has also worked with such anisotropic colloidal particles.[3] However, typical methods of synthesis do not result in sufficient quantities of particles experiencing well-characterized anisotropic interactions to study gel formation. By their nature, molecule are of narrow size distribution and typically experience anisotropic interactions. As a result, by reducing particle size to the molecular region, a wide range of systems exist with which to investigate the role of anisotropy on gel formation.

A simple model molecular system that produces gels that we have recently discovered is a binary gel formed from 1-adamantanecarboxylic acid (A1C) and 1-adamantylamine (A1N) dissolved in dimethyl sulfoxide (DMSO). Adamantane (0.6 nm in diameter) is analogous to that of a colloidal particle composed of a cage of 10 saturated carbon atoms.[5] Anisotropic interactions are introduced with the addition of side groups (in the case, a –COOH and a $–NH_3$). The adamantane core molecules will experience van der waals attractions while the amino and carboxylic acid group will experience electrostatic and acid/base

interactions. These are the classical interactions in colloidal systems. As a result, we will here explore the relationship between typical colloidal gels and molecular gels composed of adamantane molecules. In Section 3.2, we discuss our experimental system and methods of characterization; in Section 3.3 and 3.4, we present and discuss our rheological and structural findings; in Section 3.5, we present our conclusions.

### 3.2 Experimental Section

**Rheology.** Rheology measurements were performed using Bohlin rheometer at room temperature. A cone-and-plate geometry (CP $4^{o}$/40mm) with a gap space of 150mm was employed to perform amplitude sweeps. Amplitude sweep tests were performed at a frequency of 1Hz at room temperature to measure the gel's elastic modulus ($G'$) and viscous modulus ($G''$) as a function of shear stress ($\sigma$). In addition, a cap-and-bob geometry was employed to perform viscometry measurements.

**Small-Angle X-ray Diffraction/Wide-Angle X-ray Diffraction.** Both Small-Angle X-ray Diffraction (SAXS) and Wide-Angle X-ray Diffraction (WAXS) were carried out at room temperature at DND-CAT Advanced Photon Source station at Argonne National Laboratory. SAXS was used to probe a $q$-range of 0.006 to 0.165 $Å^{-1}$ , WAX was used to probe a higher $q$-range from 0.612 to 3.74 $Å^{-1}$. The X-ray wavelength and exposure time were adjusted to 1.2398 Å and 1s respectively. A custom-made sample holder consisting of rows and columns of circular discs with thickness of 0.1 cm was used. Teflon tapes were applied to both sides of the circular discs to entrap the gel inside the discs. The scattering intensity $I$ (1/cm) was measured as a function of $q$-values at each gelator volume fraction. Additional

WAXS data were acquired at Noyes X-ray facility at UIUC to capture the q-range (0.2 to 0.6 $Å^{-1}$) that was not captured at the Argonne facility. The wavelength was adjusted to 1.54 Å and a capillary tube was used as the sample holder.

### 3.3 Results and Discussion

Adamantane itself is observed to be insoluble in DMSO; however, the addition of polar groups $-NH_3$ and –COOH to adamantane renders the A1N and A1C molecules soluble in DMSO. The mixing of A1N and A1C results in acid base/electrostatic interactions that lower the solubility of the molecular complexes and subsequently drive the complexes out of solution. As reported in the previous chapter, the gel was formed at approximately 3 wt. % of A1C and A1N in DMSO. The gel is an intermediate stage between precipitation and crystallization where the molecular complexes somehow form an expanded network that could entrap DMSO and support its own weight.

For rheology measurements, we are interested in understanding both the effect of the overall volume fraction and the effect of stoichiometry on the elastic and viscous moduli ($G_o'$ and $G_o''$). Figure 7 shows $G_o'$ and $G_o''$ as a function of the mole fraction of 1-adamantylamine ($x_{A1N}$) for a 6wt.% gel. As shown, symmetry is observed in the moduli values with respect to $x_{A1N}$ and the maximum appears at $x_{A1N}$ = 0.5. The moduli values at $x_{A1N}$ = 0.25 and 0.75 (or $x_{A1C}$ = 0.25), and at $x_{A1N}$=0.42 and 0.58 (or $x_{A1C}$ = 0.42), are within the same order of magnitude. This indicates that the shear moduli depends primarily on the mole fraction of the limiting reactant in the system, whether the limiting reactant is A1N or A1C. In addition, the maximum at $x_{A1C}$ = 0.5 suggests that this binary gel is the stiffest at a 1:1 equimolar ratio of

A1N to A1C. Thus, all future rheological analysis will be performed for gels with an equimolar amount of A1N to A1C.

The effect of the overall volume fraction $\phi$ on the stiffness of the gel is explored at an equimolar ratio of A1N to A1C. Ideal mixing is assumed in the calculation for the volume fraction. The density of A1C and A1N are reported as 1.231g/ml and 1.066g/ml respectively. As shown in Figure 8, the moduli values for $G_o'$ and $G_o''$ increased from $10^2$ to $10^4$ as $\phi$ increased from 0.03 to 0.09. The moduli values increased with $\phi$ as $\sim \phi^x$, with $x \sim 4.2$ for both the elastic and viscous moduli. For a typical colloidal gel, the elastic modulus $G'$ has been found experimentally to vary with volume fraction $\phi$ through a power-law relation:

$$G' \sim \phi^{\mu},$$

where $\mu$ has values from 4 to 5.[6-7]

Similar to $G_o'$ and $G_o''$, the yield shear stress $\boldsymbol{\sigma_y}$ also vary with the volume fraction $\phi$ in a power law relation. The yield shear stress $\boldsymbol{\sigma_y}$ characterizes the shear stress at which the gel breaks down and transitions from a solid-like state to a liquid-like state (when $G' = G''$). As shown in Figure 9, the yield stress $\boldsymbol{\sigma_y}$ varies with $\phi$ as $\sim \phi^x$, with $x \sim 3.4$. For a typical colloidal gel, the yield stress $\boldsymbol{\sigma_y}$ has been experimentally found to vary with $\phi$ to the 3rd power.[8] It is important to note the striking similarity between the rheological patterns of this molecular gel and typical colloidal gels. In terms of rheological behavior, these gels exhibit characteristics similar to colloidal gels composed of particles experiencing short-range attractions.

In addition to measuring the elastic and viscous moduli of the system, we probe the viscosity of the system under shear. Figure 10 shows the viscosity measurements for gels ranging from 2.5 wt.% to 9.0 wt.%. For gels with a concentration higher than 3.0 wt.%, steady state zero viscosities ($\eta_0$)cannot be obtained. One possible reason for this is that the system is highly heterogeneous and unstable. Another plausible reason is that as the system gels, the relaxation times becomes very long, and thus the shear rate at which we would observe steady state zero shear viscosity becomes too low for us to probe. The disappearance of steady-state viscosity values at higher weight percent suggests that a gel is forming above 3% wt.

As reported in the previous chapter, the gel network is weak and is readily compressed by capillary forces. The system exhibits time-dependent behaviors. As shown in Figure 11, as a 6.0 wt.% gel is subjected to a constant oscillatory shear at 1 Hz and 3 Pa, the linear viscoelastic moduli decreased by approximately 2 folds from 3000 Pa to 1000 Pa within the hour. Therefore, when probing the system, measurements are taken for a relatively short time period before the system completely gets completely sheared down. As shown in the viscosity measurement (Figure 10), there is a stress above which the suspension experiences a dramatic drop in viscosity. Above this stress, steady-state values could be obtained. With further increase in shear stress, the system would begin shear thinning and would in theory reach $\eta_\infty$, which we expect to approach the viscosity of DMSO. However, the capability of the Bohlin rheometer is not sensitive enough to measure the viscosity of DMSO, which is 1.996 cP.

**Structure (WAXS).** Wide-angle X-ray (WAXS) was used to probe whether short-range order exists within the samples. Figure 12 shows the WAXS data for binary gels with concentration of 0.5 wt.% to 9.0 wt.%. Interestingly, several crystalline peaks were observed at each weight percent; the increase in scattering intensity of the crystalline peaks correlates with an increase in weight percent. To determine the size of the crystal domains within the gel, the Scherrer equation was used, in which,

$$\tau = \frac{\kappa\lambda}{\beta\cos(\theta)}$$

where τ is the crystal mean size, κ is the dimensionless shape factor that is close to unity, λ is the X-ray wavelength, β is the line broadening at half of the maximum intensity (FWHM), and θ is the Bragg angle of diffraction. To analyze the data, a Chebyshev's polynomial was first fitted to the data to remove the background; subsequently, the major crystalline peaks were selected manually and the crystal sizes were calculated via the Scherrer equation.

Figure 13 shows the mean crystal sizes plotted against concentration in wt.%. As shown, the crystal size does not vary significantly with an increase in A1N and A1C concentration in the gel; the average value is 34 $\pm$ 4 nm. It is interesting to point out that although we would expect the crystal size to decrease with an increase in concentration due to crowding effects, we observe that the crystals formed within the network to be independent of concentration.

To further explore this phenomenon, we experimented with the rate of mixing, drying, and the stoichiometry of the sample. For a 3.0 wt.% equimolar sample, both varying the rate of mixing and drying the sample do not have

significant effects on crystal sizes. To measure the effect of stoichiometry on crystal sizes, the stoichiometry was varied for a 5.0 wt.% sample. WAXS data was acquired at different mole fractions A1N in the gel. As observed in Figure 14, at various mole fractions ($x_{A1N}$) of A1N, the crystal sizes appear to stay constant. An overall average crystal size of 32$\pm$4 nm is observed.

From the WAXS data, we conclude that the system consists of nano-crystals. Subsequently, from a literature search of the crystal database, we deciphered the crystal packing arrangement as well as the mechanisms responsible for this arrangement. Figure 15 shows two sets of data superimposed on top of each other; as shown, the WAXS data for a 3.0 wt.% gel (shown in black) phase matched with the literature data for a single crystal of adamantan-1-ammonium 1-adamantanecarboxylate (shown in red). This indicates that the crystals formed in our gel contain the same molecular packing arrangement as that of the single crystal from the literature. As shown by the schematics in Figure 15, the unit cell for single crystal consists of eight adamantan-1-ammonium 1-adamantanecarboxylate dispiro- molecules and crystallizes in the centrosymmetric space group (s.g. C2/c, No.15).[9] An adamantan-1-ammonium 1-adamantanecarboxylate consists of a 1-adamantylammonium cation and a 1-adamantane carbonyloxy anion. The intermolecular forces responsible for crystal formation are hydrogen bonding between the ammonium hydrogen atoms and the carboxylate and the van der Waals cohesive forces among the carbon cage backbones.[9] Hence, we conclude that hydrogen bonding and van der Waals are responsible for the aggregation process of this binary gel.

**Structure (SAXS).** Small-angle X-ray (SAXS) was used to gauge whether any long-range order exist within the gel. Figure 16 shows SAXS data in scattering vector, *q,* ranging from 0.006 to 0.165 $Å^{-1}$ for gels at different concentrations. As shown, at the lower *q*-values, the scattering data follows a power-law fit that has an exponent close to -4 at all concentrations (Table 1). The exponents stayed constant despite an increase in scattering intensity due to an increase in concentration. Overall, the average value for the exponent is -3.80 $\pm$ 0.02. This scattering pattern could be explained through a surface fractal context.[9] Under a fractal context, we observe the formation of three-dimensional surface fractals in the gel. According to Porod's law at the interface boundary for a two-phase model,[10]

$$I(q) \sim q^{-(6-ds)},$$

in which the exponent of $q$ for a three-dimensional surface fractal is between -3 and -4, and $d_s$ is between 2 and 3. An exponent of 4 or $d_s$ of 2 corresponds to the limit of smooth interface boundary. Our SAXS data demonstrate $I(q) \sim q^{-3.80}$, with a $d_s$ of 2.2, which is indicative of surface fractal scattering with a sharp interface in a two-phase system that consists of the gel fibers and the solvent. The interface has a degree of roughness, or a degree of surface fractal nature. This is confirmed by the TEM image in Figure 17a, in which we observe slight roughness on the fibers' surfaces.

In addition, as observed from the SAXS data, the slope of the intensity curves do not appear to level off even at the lowest q-values measured. In here, the lowest q-value is around 0.006 $Å^{-1}$, which correlates with a real-space size of ~100nm, suggesting that the size of the aggregates in here is at least 100nm. As reported previously, TEM images suggests that the diameters of the fibers vary anywhere

from thin strands of 200nm to large bulky ones of $\geq$1um. Both the SAXS data and TEM images indicate the presence of large structures.

The effect of stoichiometry was also explored using the SAXS data. As shown in Table 2, varying the stoichiometry did not have marked effect on the degree of roughness, or magnitude of the surface fractal dimension of the fiber. The average value of the exponent is again -3.80$\pm$0.02, or a $d_s$ of 2.2. For both the SAXS and WAXS data, changing the stoichiometry does not effect either the degree of roughness or the size of the crystallites.

**Gel Composition.** SAXS, TEM, and DLS, data demonstrate that our system consists of large and branched fibers with a somewhat rough interface. we attempt to answer this question by presenting a schematic of the aggregation scheme in Figure 18. As shown, at first, A1N and A1C molecules would aggregate via hydrogen bonding and van der Waals forces into 20-30nm crystallites, which would then further aggregate with random orientation into large crystalline fibers. These fibers would then align to trap the solvent and thus forming a self-supporting network. This idea of ~30nm crystallites aggregating into fibers is also supported by the TEM image displayed in Figure 17b. From the image, we observed what appeared to be 30-50nm sized aggregates inside the fibers. However, again, even though the sizes matches well with the size of crystallites, we cannot state for certain whether the fibers consist solely of crystallites, or a combination of amorphous aggregates and crystallites. The WAXS data indicate that the fibers are composed of ~30nm crystallites. The independence of the crystallite size on stoichiometry, rate of

mixing and rate of drying indicate this characteristic size is set by physical processes independent of these parameters.

To answer this question, we performed WAXS on a 3 wt.% sample in a holderless setup. For this setup, the gel is suspended on a small ring in a thin film and so the X-ray could shoot through the sample without any interference or scattering from the holder. Figure 19 shows the raw data for the 3 wt. % sample. Both sharp crystalline peaks and a big amorphous peak are observed in the data. The crystalline peaks, as stated before, correlate with the nano-crystals formed by A1N and A1C; the amorphous peak, on the other hand, correlates with the solvent DMSO scattering. The total area under all the peaks measures the total amount of material that can scatter. While the area under the sharp crystalline peaks is proportional to the amount of crystals within the system, the area under the big amorphous peak is proportional to the amount of scattering due to the solvent DMSO. By comparing the area under the crystalline peaks to the total area under all peaks, we could approximate the degree of crystallinity in the system. For this particular 3 wt.% sample, the degree of crystallinity in the sample is 2.3%, indicating that a majority of the 3 wt.% materials in the sample exists in the form of crystallites. Based on this experiment, we could generalize that most of the aggregates inside the fibers are crystalline in nature.

**Crystals.** Another challenge is to understand why the crystallites would stop growing at a certain size despite variations in concentration, mixing rate, drying, and even stoichiometry. Is this similar to a nucleation phenomenon where once the aggregates reach a certain critical size, they would stop growing? Or could it be that

our methods of analysis is not rigorous enough to capture the small changes in crystallites sizes with respect to concentration? For instance, as shown in Figure 19, the amorphous peak of DMSO overshadows the crystalline peaks, which may become a problem because we need to manually select the crystalline peaks. This would generate some degree of uncertainty in the calculation for crystal sizes.

Suppose that as suggested by Figure 18, the 30~40 nm crystallites subsequently aggregate into fibers. Then, another critical question left to be unanswered is 'how' do these crystallites assemble into fibers? What gives these crystals the anisotropic preference for aggregating uniaxially instead of isotropically into a sheet or some other structures? What defines the size of these fibers and how do these fibers rebuild after shear? These are some of the critical questions left to be answered.

**Comparison.** Finally, the most intriguing yet fascinating phenomenon observed in this system is the agreement between in the gel's rheological behavior and that of a typical colloidal gel. In a typical gel, $G'$ would vary with $\phi^{\mu}$, where $\mu$ is between 4 and 5; and the yield stress $\sigma_y$ would vary as $\phi^{3.0}$. In this system, $G' \sim \phi^{4.2}$ and $\sigma_y \sim \phi^{3.4}$. However, the structure of the gel in a colloidal system differs vastly from that of this binary gel. Colloidal gels typically consist of mass fractal aggregates, which are open and branched structures that aggregate further into a gel. However, in the case of this binary gel, we observed an interwoven and branched fibrous network that is typical of molecular gels. Despite the two vastly different structures, the rheological patterns are similar. This could suggest one of

the two things: first, that this is indeed a mere coincidence; secondly, that this binary gel is fundamentally similar to a typical colloidal gel. Supporting evidence for the second scenario includes both TEM and WAXS date where we observe that the system consists of 30-50 nm crystallites; thus, perhaps we could treat these aggregates as fractals similar to those in colloidal systems. As a next step, we will try to better understand this system and apply other existing colloidal theories to this system for further comparison with colloidal gels.

### 3.4 Conclusion

The rheological and structural properties of this binary gel have been discussed and analyzed. Gel rheology, namely, the power –law dependence of moduli and yield stress on volume fraction, resemble that of a typical colloidal gel. Both vary as $G' \sim \phi^x$ and $\sigma_y \sim \phi^y$, where $x$ is approximately 4-5 and $y$ is ~3. This binary gel is composed of fibrous networks as opposed to the fractals observed in colloidal gels. In addition, the gel appeared to be composed of ~30nm crystallites which aggregate into fibers to entrap the DMSO and form a gel. The intermolecular forces responsible for gel formation are hydrogen bonding and van der Waals forces. The crystallites experience anisotropic interactions necessary for these particles to assemble into fibers. The gel stiffness depends on the limiting reactant (A1C or A1N) in the system and the gel is the stiffest at a 1:1 equimolar amount of A1C to A1N. Under sufficiently large stress, the gels yield and shear thin. Upon the cessation of flow, the elastic modulus partially recovers.

There are several important questions that need to be addressed. For instances, it was observed that the size of the crystallites does not depend on either

the concentration, the mixing rate, the drying process, or the stoichiometric ratio. It is little understood why this would be the case and future studies will necessary to better understand this phenomenon. We believe that the crystallites would undergo a second aggregation to form strands of fibers with diameters ranging from 200nm to $\geq$1μm. Again, we still do not fully understand the mechanisms for this aggregation and why the crystallites would have an anisotropic preference for aggregation. These are some of the critical questions that needs to be answer in the future.

### 3.5 Tables and Figures

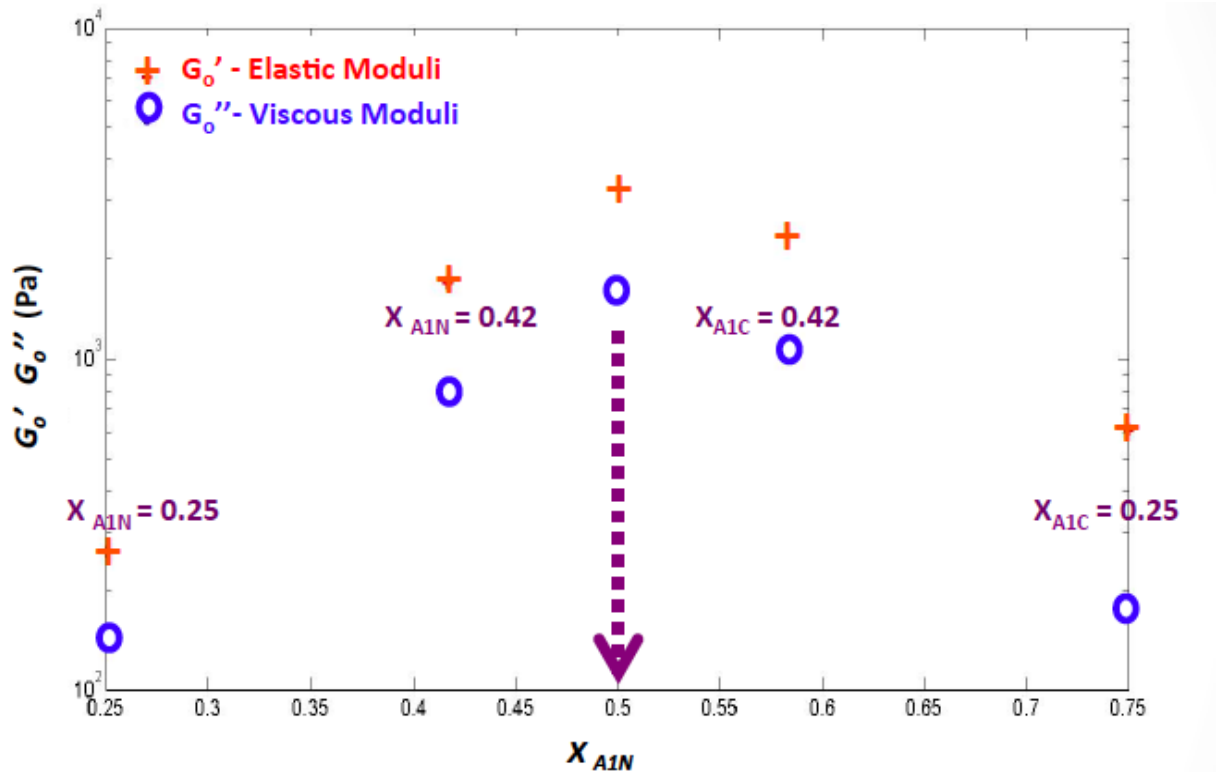


**Figure 7. The $G_o$' and $G_o$" values plotted against mole fraction of A1N ($x_{A1N}$) for gel at 6 wt.%. Symmetry is observed for moduli values as a function of $x_{A1N}$; maximum moduli values are observed at $x_{A1N}$ =0.5.**

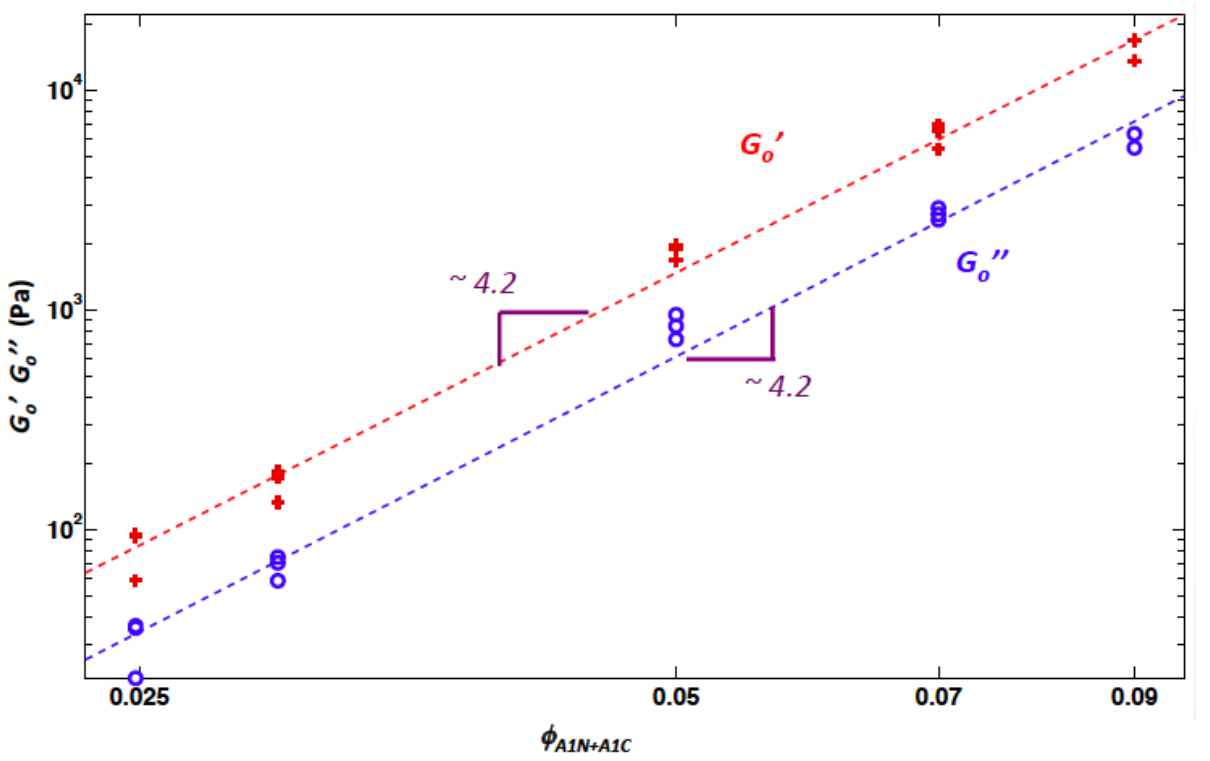


**Figure 8. $G_o'$ and $G_o''$ were plotted against $\phi_{A1N+A1C}$ in a log-log plot with $\phi_{A1N+A1C}$ = 0.025, 0.03, 0.05, 0.07, and 0.09. The data points were fitted to a power law and the exponent is 4.15 for both for $G_o'$ and $G_o''$.**

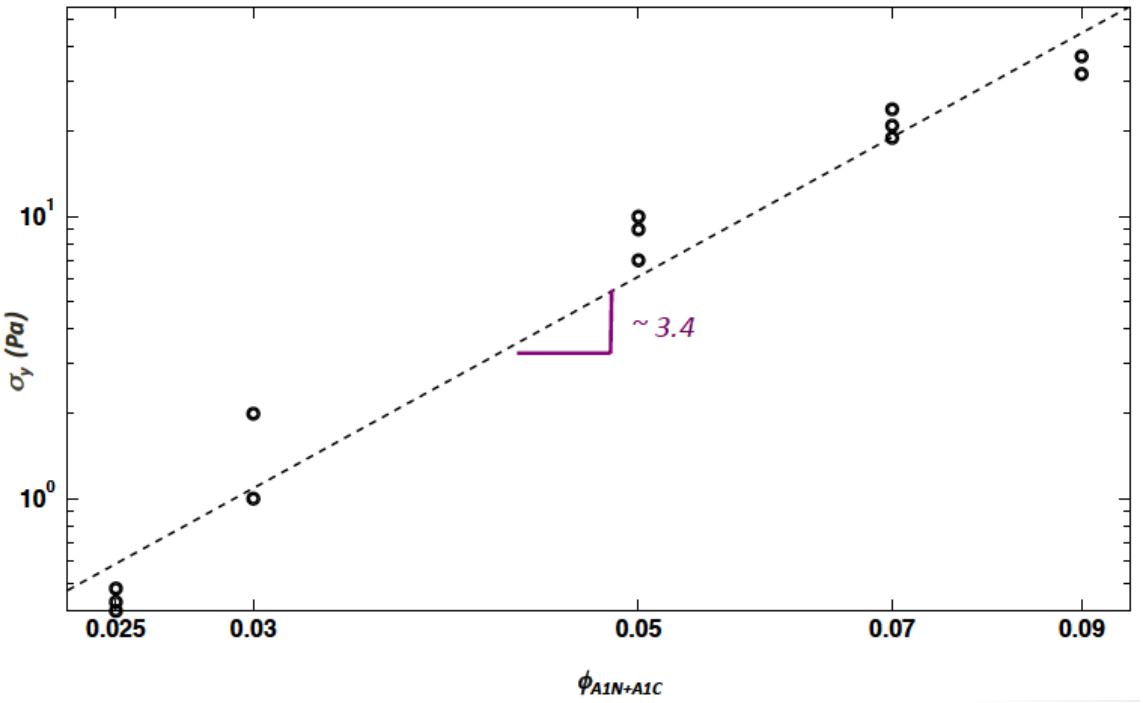


**Figure 9. The yield stress $\sigma_y$ was plotted again gel weight fraction in a log-log plot and fitted to a power law of $\phi_{A1N+A1C}$ to the 3rd power.**

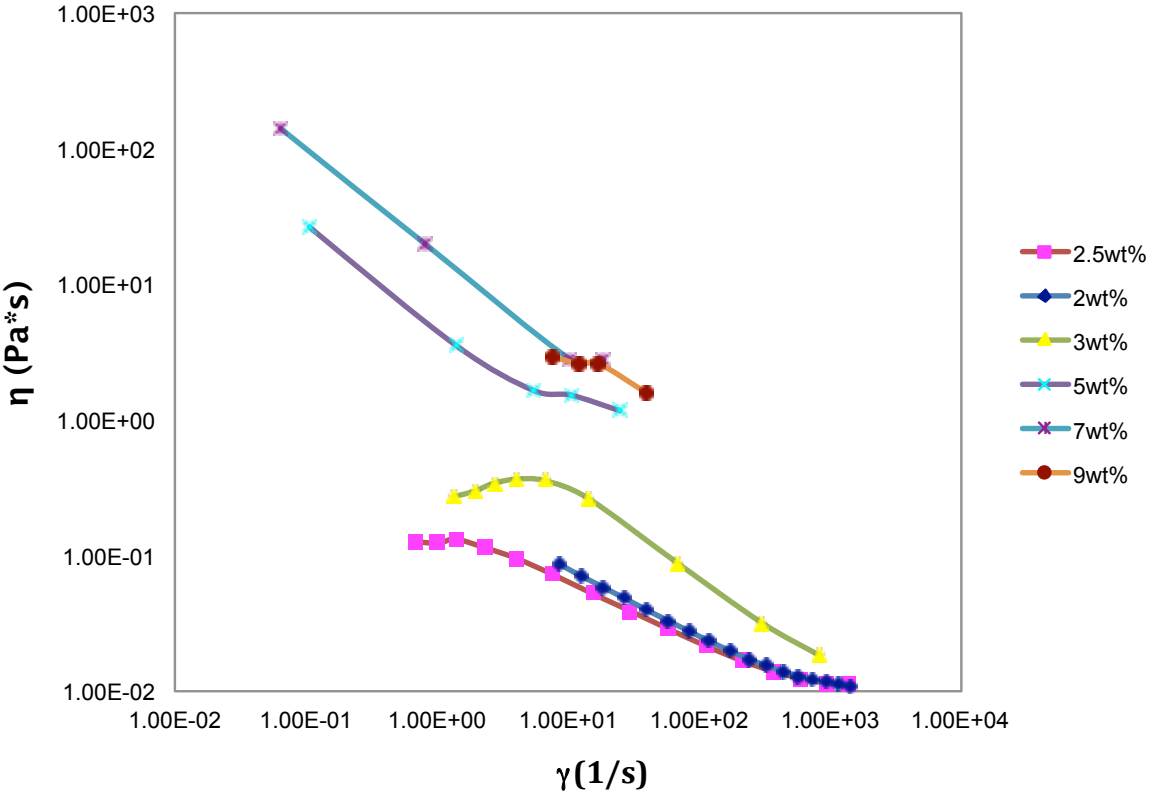


**Figure 10. Viscosity data for concentrations from 2wt% to 9wt%. Steady state values are reached at shear rate $\gamma \geq 0.1/s$. Shear thinning is observed as $\gamma$ increases.**

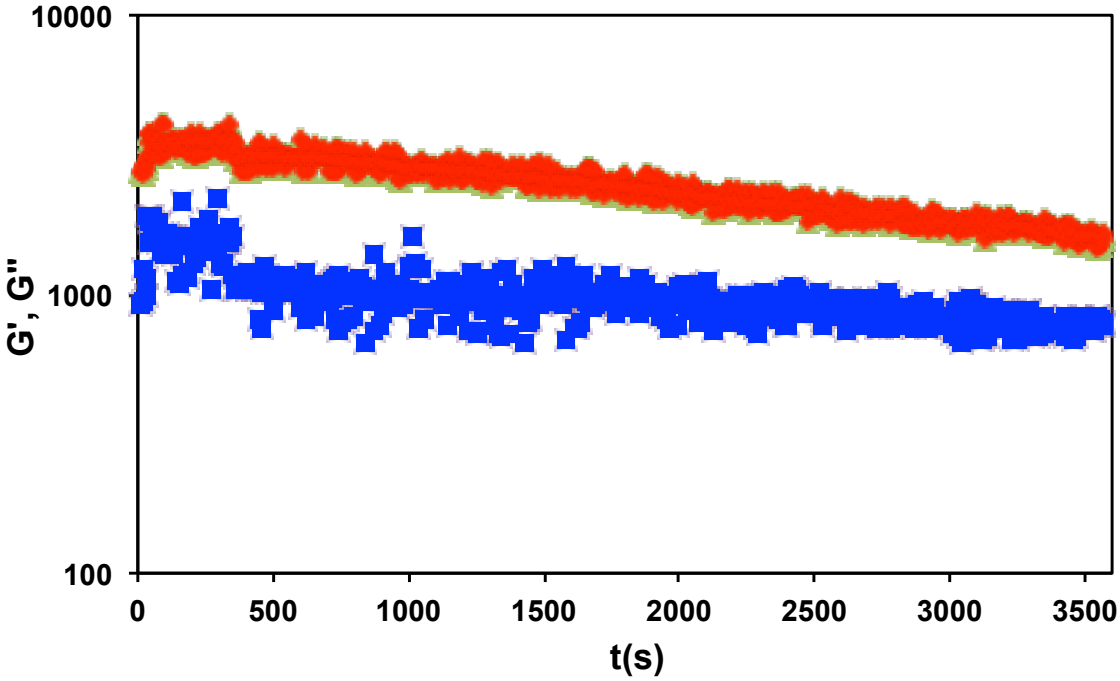


**Figure 11. Time-dependent behaviors of the gel moduli.**

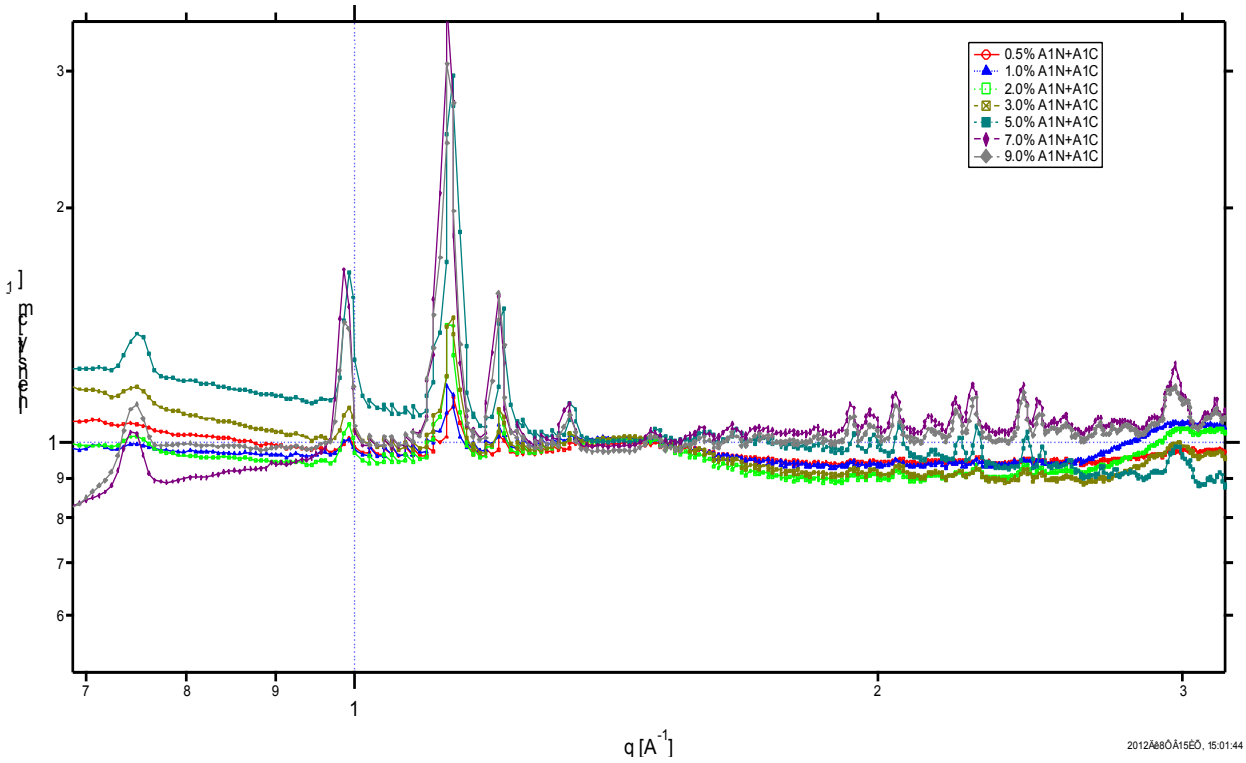


**Figure 12. WAXS data for gels at various concentrations (0.5 wt.% to 9.0 wt.%) with the scattering intensity measured as a function of q-values in the range of 0.612 to 3.74 Å$^{-1}$ The peak sizes increased with an increase in concentration of gelator molecules.**

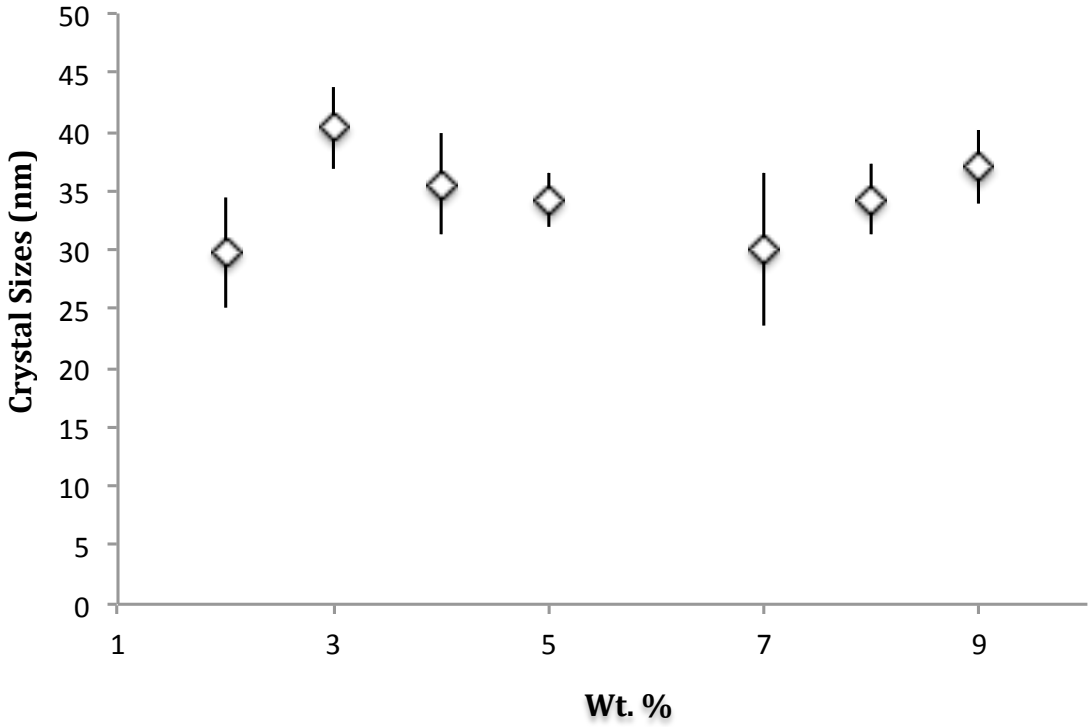


**Figure 13. The crystal sizes calculated from the Scherrer equation are plotted as against wt.% for gels an equimolar amount of A1N to A1C. The sizes range from 30 to 40 nm and so apparent trend was observed for crystal sizes with respect to the overall weight percent. The overall average size for crystals is 34.4±3.9 nm.**

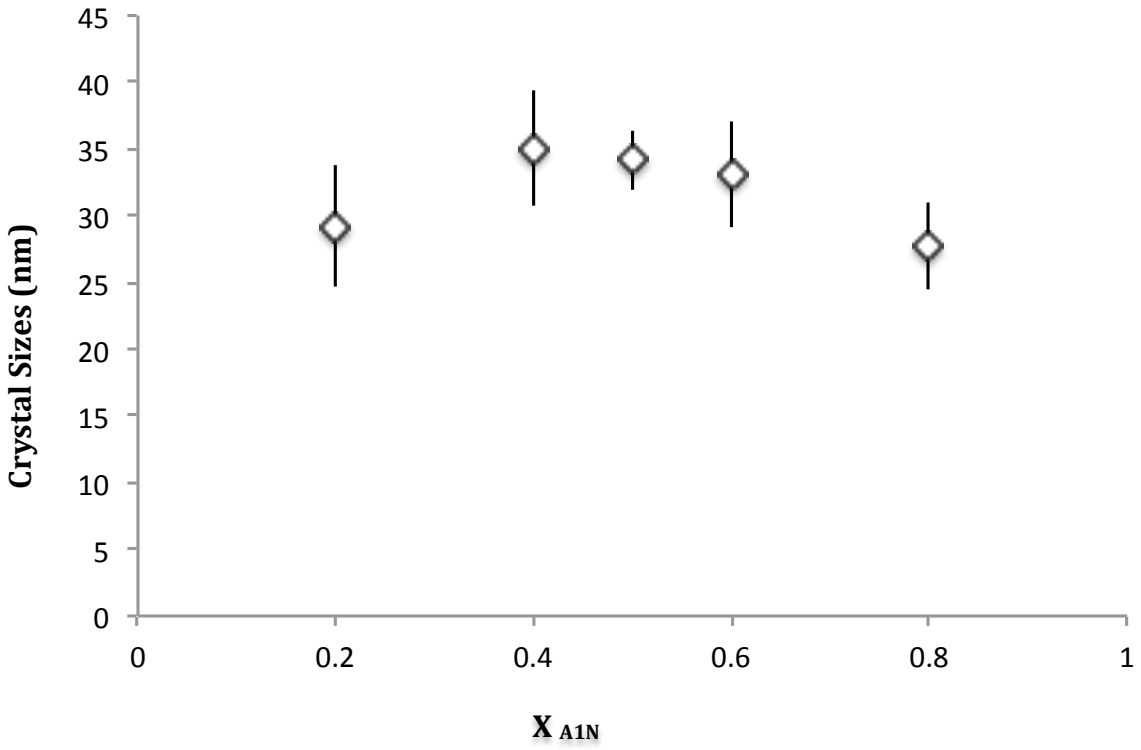


**Figure 14. The crystal sizes calculated from the Scherrer equation are plotted as against various mole fractions of A1N ($x_{A1N}$) for 5 wt.% gels. Again, the crystal sizes are independent of the A1N mole fraction; an overall average crystal size of 31.9±3.9 is observed.**

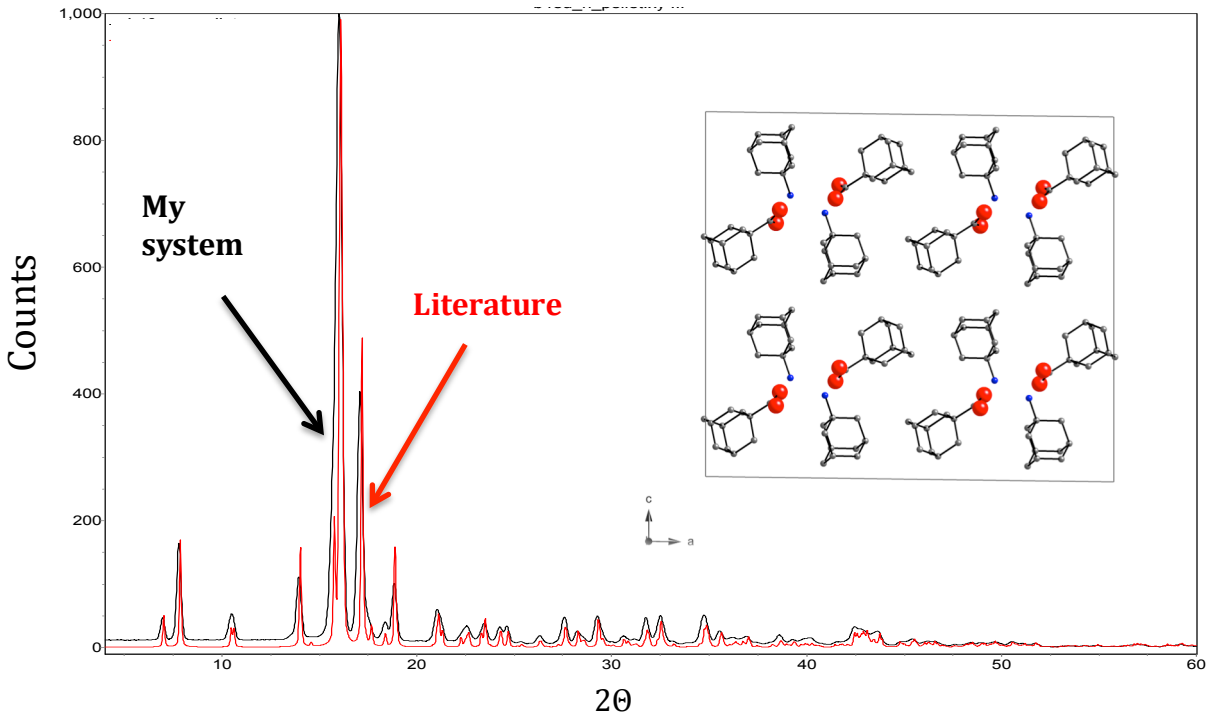


**Figure 15. WAXS data for a 3 wt.% gel (shown in black) phase-matched with the single crystal data for adamantan-1-ammonium 1-adamantanecarboxylate (shown in red). Shown in the right hand corner is the unit cell depiction for a single crystal data of adamantan-1-ammonium 1-adamantanecarboxylate compound. Its unit cell consists of eight dispiro adamantan-1-ammonium 1-adamantane-carboxylate molecules. (Oxygen molecules are shown in red; nitrogen molecules are shown in blue; hydrogen molecules are omitted in this figure).**

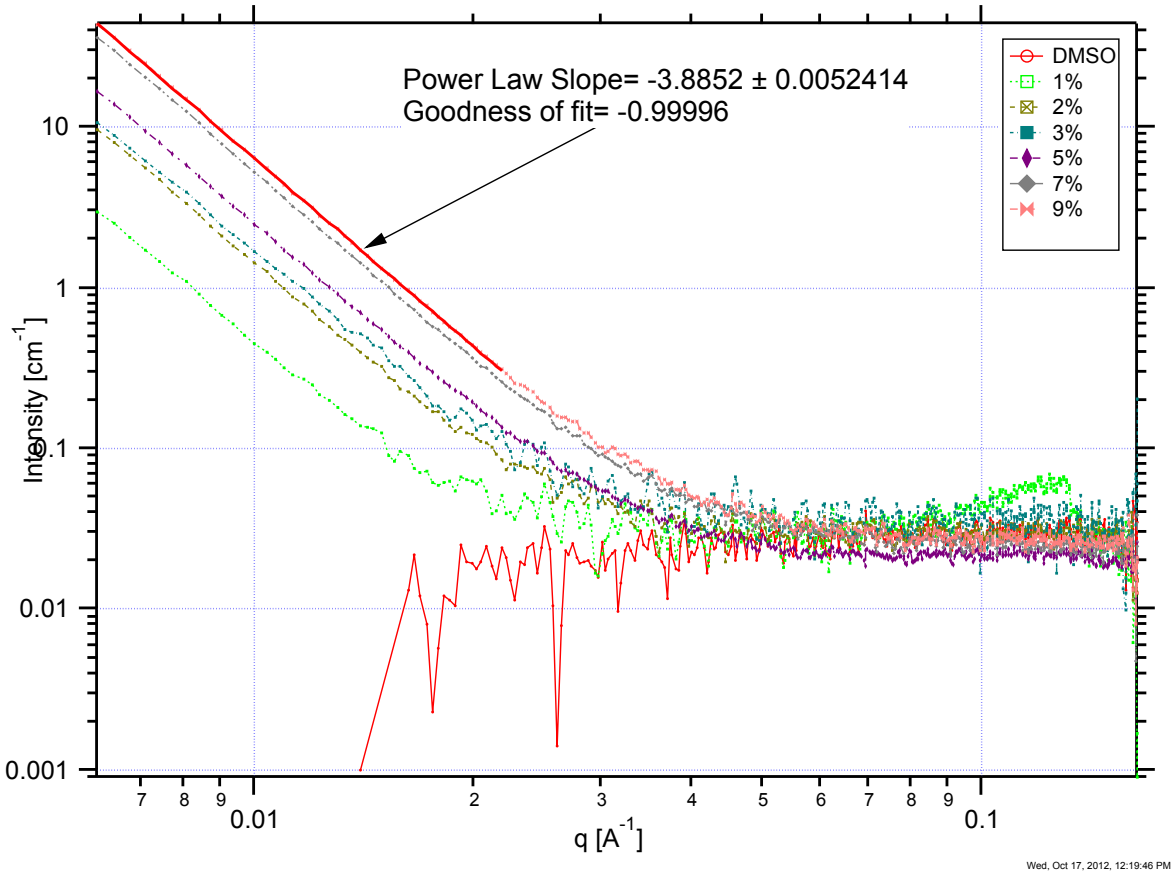


**Figure 16. SAXS data for gels at various concentrations (0.5% to 9.0wt%) with scattering intensity measured as a function of q-values in the range of 0.007 to 0.15 Å$^{-1}$. The scattering intensity was observed to shift up uniformly with increase in concentration. A power-law fit was applied to low q-values at each concentration and the slope was tabulated in Table 1.**

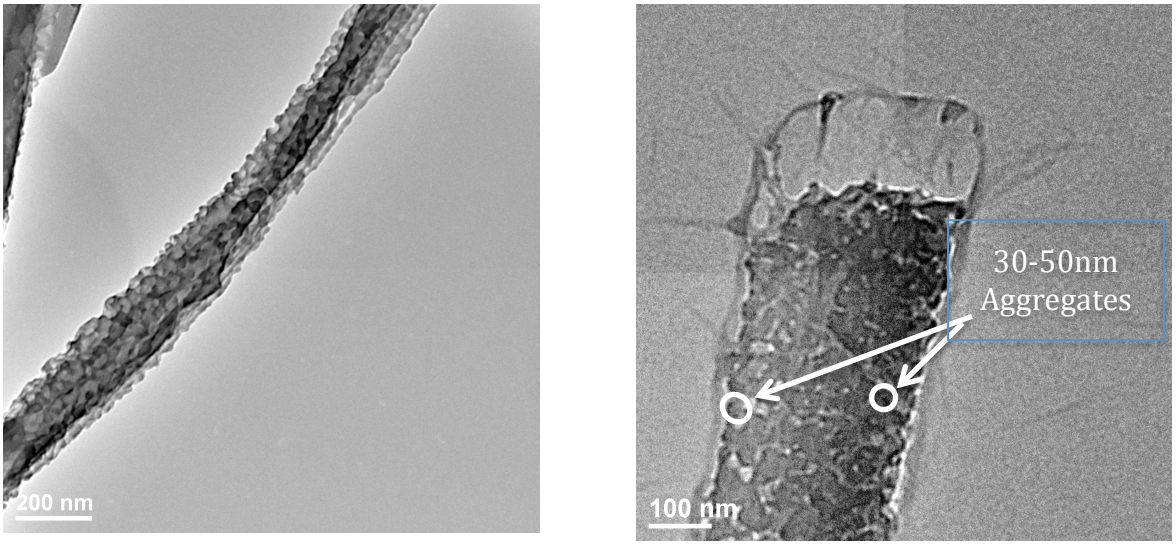


**Figure 17. a) TEM image showing a single fiber with a slightly rough surface b) Small aggregates with size of 30-50 nm are observed in the enlarged view of the internal structure of a fiber.**

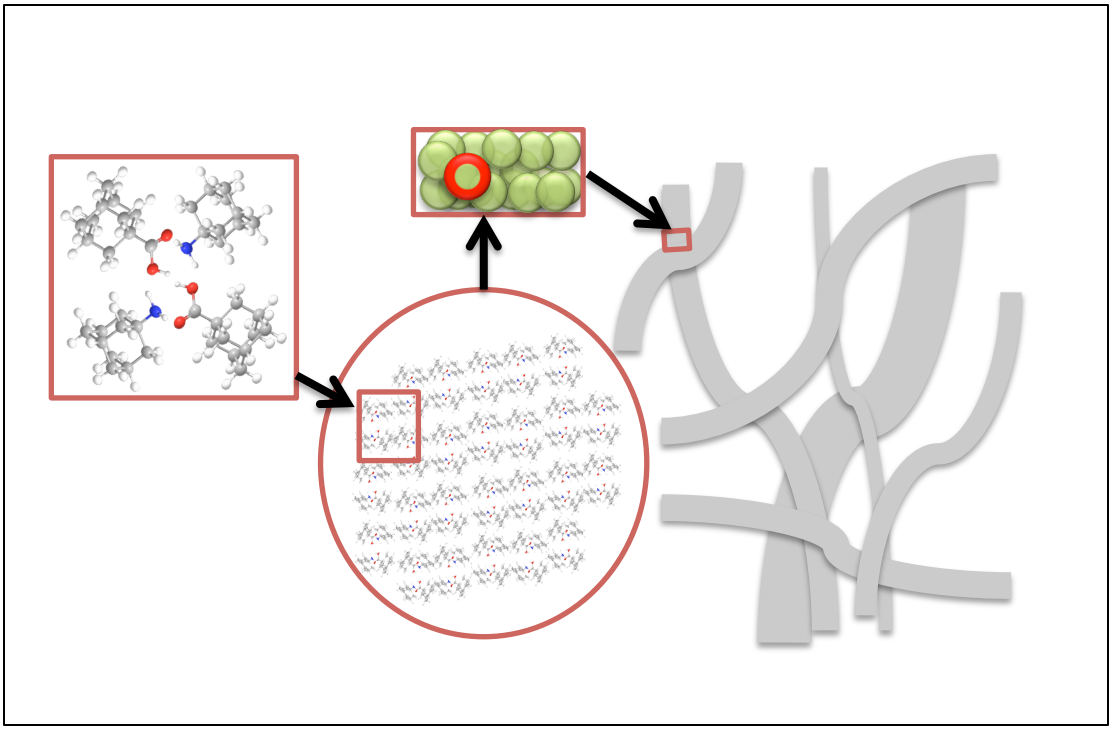

**Figure 18. Schematic of the gel's aggregation scheme: A1C and A1N first aggregate into ~30nm crystallites, which further aggregate into fibers with varied diameters (200nm to ≥1μm).**

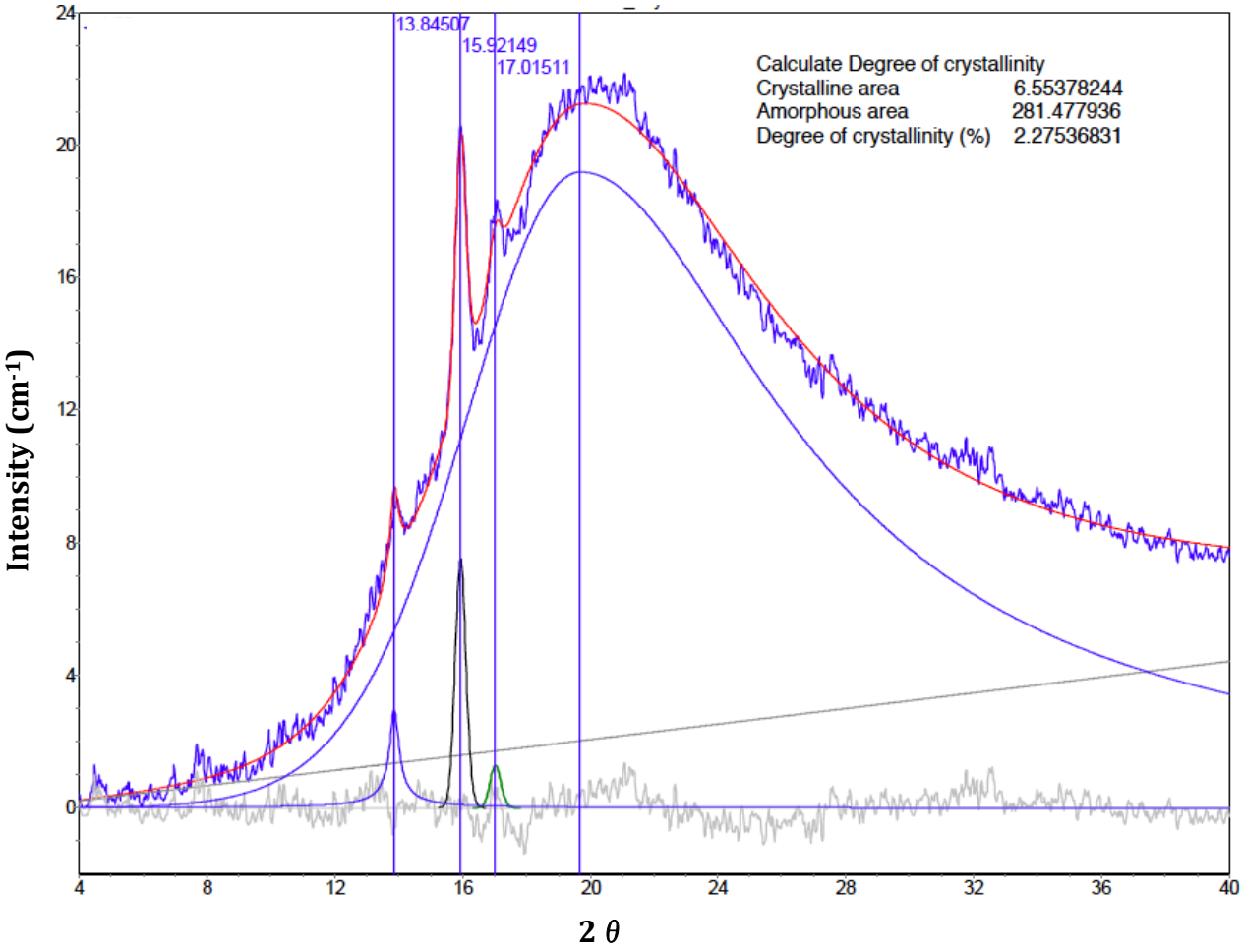


**Figure 19. Raw WAXS data showing both the amorphous contribution from DMSO and crystalline contribution from A1C and A1N. The degree of crystallinity can be calculated by dividing the crystalline area under the peak to the total area.**

**Table 1. Exponent *x* for the Power-law fit of intensity versus *q*-values ($I \sim q^x$) at different weight percent of equimolar A1N and A1C in solution**

| Wt.% | Exponent | Standard Deviation |
|---|---|---|
| 1 | -3.66 | 0.03 |
| 2 | -3.85 | 0.01 |
| 3 | -3.69 | 0.02 |
| 5 | -3.79 | 0.01 |
| 7 | -3.89 | 0.01 |
| 9 | -3.89 | 0.01 |

**Table 2. Exponent *x* for the Power-law fit of intensity versus *q*-values ($I \sim q^x$) at different mole fractions of A1N for a 5 wt.% gel**

| $X_{A1N}$ | Exponent | Standard Deviation |
|---|---|---|
| 0.2 | -3.91 | 0.02 |
| 0.4 | -3.60 | 0.02 |
| 0.5 | -3.79 | 0.01 |
| 0.6 | -3.90 | 0.01 |
| 0.8 | -3.80 | 0.02 |

### 3.6 References

(1) Zaccarelli, E. Colloidal Gels: Equilibrium and Non-Equilibrium Routes. *J. Phys.: Condens. Matter,* **2007**, 19, 323101.

(2) Russell, E., Sprakel, J., Kodger, T.E., Weitz, D.A., Colloidal Gelation of Oppositely Charged Particles. *Soft Matter.* **2012**, 8, 8697.

(3) Jiang, T., Zukoski, C.F. Synthesis of pH-Responsive Particles with Shape Anisotropy. *Langmuir,* **2012**, 28 (17), 6760-6768.

(4) Wang, Y., Breed, D.R., Manoharan, V.N., Feng, L., & … Pine, D.J. Colloids with Valence Specific Directional Bonding. *Nature* **2012**. 491(7422), 51-55.

(5) Morel, J.-P.; Morel-Desrosiers, N. Standard Molar Enthalpies and Volumes of Adamantane in Methanol, Ethanol, Acetone, and n-Dodecane. Interpretation using Scaled Particle Theory. *J. Solution Chem.* **1981**, *10(6),* 451-458.

(6) R. Buscall, P.D. A. Mills, J.W.Goodwin and D.W.Lawson, Scaling behavior of the rheology of aggregate networks formed from colloidal particles. *J Chem Soc, Faraday Trans* **1988**, 84, 4249-60

(7) Rueb, C.J., Zukoski, C.F., Viscoelastic properties of colloidal gels. *J. Rheol.,* **1997**, 41(197).

(8) M.Chen and W.B. Russel, Characteristics of flocculated silica dispersion. *J Colloid Interface Sci.* **141** (1991), 564-77.

(9) Mullica, D. F.; Scott, T. G.; Farmer, G. M.; Kautz, J. A.; Structure of adamantan-1-ammonium 1-adamantanecarboxylate. *J. Chem. Crystallogr.* **1999**, *29(7),* 845-848.

(10) Roe, R.-J. *Methods of X-Ray and Neutron Scattering in Polymer Science;* Oxford University Press: New York, 2000.

# CHAPTER 4. CONCLUSION

## 4.1 Summary

The topic of my master's thesis is the formation and properties of diamondoid molecular gels. The motivation behind this work is to i) discover a model molecular system that gels, and to ii) compare its rheological behaviors with those of known colloidal gels. The hypothesis we explore is that molecular gels and colloidal gels are fundamentally similar, with the only exception that molecules are much smaller than colloidal particles.

The molecule of choice is adamantane, a $C_{10}$ caged saturated carbon molecule that is globular in nature just like a colloid, but smaller (0.6 nm). This molecule has the advantages that: i) it is readily available, and ii) interactions can be made anisotropic and gel behavior controlled by introducing side chains to control strength of interaction. The approach we took was to look for a system where the molecules are soluble and then establish a trigger that increases the strength of attraction, drives aggregation and/or decreases solubility. This was done by working with two adamantane molecules: 1-adamantanecarboxylic acid (A1C), and 1-adamantylamine (A1N). While adamantane alone is insoluble in DMSO, due to the polar moieties attached, both of these molecules are highly soluble in DMSO. The van der Waals attractions and lack of attraction between the DMSO and the particle is insufficient to solubilize an underivitized adamanatane. However, due to polar interactions, A1N and A1C are soluble in DMSO. When solutions of A1N and A1C are mixed, aggregates are formed and the solutions turn turbid. For a 1:1 ratio of A1N to

A1C, gels are formed at a total adamantane concentration of approximately 3.0 wt.%.

Transmission electron microscopy (TEM), dynamic light scattering (DLS), small-angle and wide-angle scattering (SAXS and WAXS) demonstrate that the solids formed on mixing the two DMSO solutions consist of fibers with diameters and lengths ranging from several hundred nanometers to $\geq$ 1μm. These fibers have slightly rough surfaces and are composed of ~30 nm diameter crystallites. The scattering pattern indicates that these crystals are formed. The crystallites must experience anisotropic interactions enabling them to aggregate into fibers that branch and entangle until they fill space and thus form a gel. The data are consistent with a scheme where gels are formed via i) A1C and A1N molecules aggregate via intermolecular forces into ~30nm crystallites, which then ii) further aggregate into interwoven and branched fibers of various sizes, that iii) trap DMSO to form a self-supporting gel network.

The rheology of the binary gel indicates that for the range of frequency studied, the gel's linear moduli are to be independent of strain frequency for two orders of magnitude (0.1 to 10Hz). The linear elastic moduli *G', varies as* $\sim \phi^{4.2}$ and the yield stress $\sigma_y$, determined from a stress sweep at 1Hz, varied with $\sim\phi^{3.4}$. These power law dependences are typical to those of colloidal systems. The gels shear thin at stresses larger than the yield stress and upon cessation of stress, the mechanical properties are partially recoverable.

We conclude that while composed of small molecules, the gel responds mechanically like a colloidal gel. The structure of this gel, however, is strongly

influenced by anisotropic interactions of the constituent molecules with its fibrous structure typical for molecular gels. It appears that this binary system represents a system that is a mixture of crystallization, precipitation, and gelation.

### 4.2 Future Studies

There are several important questions that need to be addressed in future studies. First of all, the physical chemistry controlling crystallite size and aggregation are poorly understood. The crystallite size is weakly dependent on aggregation conditions.

The second major area of study is how these crystallites assemble into fibers. Of interest here are the nature to the crystallite interactions giving rise to fibers, and understanding what dictates the width and length of the resulting fibers. These are all interesting questions about the gel's structural properties that are waiting to be unraveled.

We are also interested in understand how the structure of the system is altered by the application of shear and subsequently, how the structure rebuilds. For instance, do these fibers break off, and then randomly reattach to other fibers to rebuild? Or do the fibers gets shear down even to smaller components, perhaps all the way to its ~30nm crystallites, which then reassemble randomly into fibers?

Finally, we are curious to see whether this particular system can be treated like colloidal systems. Its rheological behaviors (G' and $\sigma_y$ dependence on $\phi$) are surprisingly similar to that of colloidal gels. In addition, from what we've gathered, even though the gel is composed of fibrous networks, the fundamental building

blocks appear to be ~30nm crystallites. Then, can we treat these crystallites as fractals like the fractals in colloidal gels? To answer this question, we could attempt to apply other existing colloidal theories to this binary gel and check the applicability of these theories. An example of such theories is the Modified Mode-Coupling Theories (MCT) developed by Schweizer et al. This theory can be used to predict gel properties, including the elastic moduli $G'$, the point of gelation $\phi_{gel}$, and the localization distances $r_{loc.}$, which control the systems mechanical porperties.[1-4]

**4.3 References**

(1) Chen, Y.L.; Schweizer, K.S. J. Microscopic theory of gelation and elasticity in polymer-particle suspensions. *Chem. Phys.* **2004,** 120 (7212).

(2) Bergenholtz, J.; Fuchs, M. Gel transitions in colloidal suspensions. *J. Phys.; Condens. Matter* **1999,** 11(10171).

(3) Schweizer, K.S.; Saltzman, E.J. Entropic barriers, activated hopping, and the glass transition in colloidal suspensions. *J. Chem. Phys.* **2003,** *119* (1181).

(4) Ramakrishnan, S., Zukoski, C.F., Microstructure and Rheology of Thermoreversible Nanoparticle Gels, *Langmuir,* **2006,** 22(7833-7842).